Int. J. Electrochem. Sci., 10 **(2015)** 8844 - 8857

International Journal of
ELECTROCHEMICAL
SCIENCE
www.electrochemsci.org

Short communication

Preparation of a trimetallic $Pd_1Ni_yAl_{0.5}$ composite nanoparticle by a hydrothermal method for ethanol oxidation reaction

Keqiang Ding[*], *Yuan Li, Yongbo Zhao, Jing Zhao, Yuying Chen, Qingfei Wang*[*]

College of Chemistry and Materials Science, Hebei Normal University, Shijiazhuang 050024, P.R. China
[*]E-mail: dkeqiang@263.net; wqfxt@126.com

Received: 31 July 2015 / *Accepted:* 25 August 2015 / *Published:* 30 September 2015

A series of trimetallic $Pd_1Ni_yAl_{0.5}$ composite nanoparticles (the nominal atomic ratios of Pd:Ni:Al were 1:2:0.5,1:4:0.5 and 1:6:0.5, respectively) were produced onto multi-walled carbon nanotubes (MWCNTs) (denoted as $Pd_1Ni_yAl_{0.5}$/MWCNTs) using a hydrothermal process. The crystalline phases and morphologies of the samples were mainly featured using X-ray diffraction (XRD), scanning electron microscope (SEM) and transmission electron microscopy (TEM). Ethanol oxidation reaction (EOR), an important anodic reaction in direct ethanol fuel cells (DEFCs), was examined on the as-prepared catalysts principally by using cyclic voltammetry (CV) and chronoamperometry (CA), and the results demonstrated that the catalyst of $Pd_1Ni_4Al_{0.5}$/MWCNTs showed the best electrocatalytic performance among all the prepared samples. The relatively smaller particle size and higher polarized electrode potential were regarded as the major reasons for the excellent electrocatalytic activity of the $Pd_1Ni_4Al_{0.5}$/MWCNTs towards EOR in comparison with other catalysts.

Keywords: hydrothermal process； $Pd_1Ni_yAl_{0.5}$ trimetallic nanoparticles； ethanol oxidation reaction; electrocatalysis

1. INTRODUCTION

Although hydrogen gas based proton exchange membrane fuel cells (PEMFCs) have received enormous interest owing to their unique properties such as high energy conversion efficiency and zero emission, the safety issue (especially in the transportation and storage process) still greatly hindered their further real applications [1]. Thus, direct alcohol fuel cells (DAFCs) are considered very attractive energy conversion systems thanks to their unique advantages like elevated energy density, high conversion efficiency, adaptability to portable devices and low-temperature operation [2]. Direct

methanol and ethanol fuel cells (DMFCs and DEFCs) are the main two kinds of DAFCs. Compared with methanol, ethanol possessed many superior properties such as high energy density and lower toxicity. Most importantly, ethanol could be produced massively from agricultural products by fermentation. Therefore, ethanol oxidation reaction (EOR) has become into a hot topic in the research field of electrochemistry [3].

It is well known that platinum (Pt)-based electrocatalysts are the most widely used catalysts for EOR in DEFCs. Except for the high cost and limited supply of Pt, it was also revealed recently that the kinetics of EOR on Pt was very sluggish and the complete oxidation of ethanol is difficult to achieve [4]. Hence, developing novel catalysts for EOR is crucial for the further applications of DEFCs. Of late, it was demonstrated that palladium (Pd) is a good electro-catalyst for ethanol oxidation especially in alkaline media. Therefore, Pd and Pd-based electrocatalysts are extensively studied mainly owing to its similar electronic structure, lower cost and more abundance on the earth when compared with Pt [5].

Combining Pd with another two kinds of metal to prepare a trimetallic catalyst is one of the most effective ways to promote the electrocatalytic ability of a pure Pd catalyst while lowering its utilization. Although a large number of papers concerning the Pd-based electrocatalysts for EOR have been published, the reports focusing on the preparation of the Pd-based trimetallic nanocatalysts for EOR are rare. For example, Viswanathan et al.[6] prepared carbon black supported Pd-Co-Mo alloy nanoparticles by a chemical reduction method using hydrazine as the reductant, and the resultant catalysts were applied towards oxygen reduction reaction (ORR). He pointed out that the ORR activity of heat-treated Pd-Co-Mo was comparable to the commercial Pt. Li et al.[7] proposed a simple and controllable *in situ* chemical method for preparing palladium/tin oxide-titanium dioxide/multi-walled carbon nanotube (Pd/SnO_2-TiO_2-MWCNTs) catalysts for direct formic acid oxidation. And he thought that the synergetic effect between the Pd and Sn oxides should be responsible for the enhanced electrocatalytic performance exhibited by this novel kind of catalyst. Czerwiński's group [8] fabricated Pt-Rh-Pd electrodes on a gold wire by using a potentiostatic electrodeposition method from chloride solutions, and then methanol adsorption and electrooxidation were thoroughly examined on the as-prepared electrodes. Liao et al.[9] described a novel method of a pulse electrodeposition process for synthesizing an core-shell structured AuPt@Pd/C catalyst for the electrooxidation of formic acid. He found that an excellent activity towards the anodic oxidation of formic acid was displayed by this novel catalyst when compared to commercial Pd/C. Very recently, Abruňa et al. [10] prepared electrode arrays, that mainly contained Pt-Sn-M (M =Fe, Ni, Pd, and Ru), via a borohydride reduction of aqueous metal salts on carbon paper, he confirmed that four kinds of the as-synthesized catalysts were significantly more active than Pt or PtSn catalysts. Although several kinds of Pd-based trimetallic composite or alloyed particles have been prepared as shown above, to the best of our knowledge, no paper reporting the preparation of Pd-Ni-Al ternary nanoparticles was published so far.

Recently, some novel types of carbon like graphene [11] and nanofiber [12] have been prepared, however, carbon nanotubes (CNTs), due to its unique properties such as high specific surface area, low resistivity, and good thermal and chemical stability, still received increasing interest [13]. Usually, metal nanoparticles could be immobilized onto CNTs by using an chemical reduction method, namely, metal precursors were reduced by a reducing agent to generate metal atoms (particles) on the

surface of CNTs. In this work, only metal precursors, MWCNTs and distilled water were contained in the reacting system, and no other reducing agents were introduced. To our knowledge, except our previous work [14], the works of using MWCNTs as the reducing agent to prepare metal nanoparticles onto the surface of MWCNTs are rarely reported.

In this paper, three kinds of $Pd_1Ni_yAl_{0.5}$/MWCNTs nanocomposite catalysts with different atomic ratios were synthesized by a facile method of hydrothermal process, in which only metal precursors, distilled water and MWCNTs were contained. Transmission electron microscopy (TEM), scanning electron microscopy (SEM) and x-ray diffraction (XRD) were used to feature the morphology and crystalline structures of the as-prepared $Pd_1Ni_yAl_{0.5}$/MWCNTs. Cyclic voltammetry (CV) and chronoamperometry (CA) were mainly employed to examine the electrochemical activities of the as-prepared catalysts for EOR. Developing a novel catalyst for EOR was the main contribution of this work, which is believed to be beneficial to the development of EOR catalysts.

2. EXPERIMENT

2.1 Materials

MWCNTs (purity>95%) with an average diameter of 10-20 nm were bought from Shenzhen nanotech port Co., Ltd. **(**China). All the electrodes were ordered from Tianjin Aida Co., Ltd (China). All the chemicals were of analytical grade and used as-received without any further treatment. Doubly distilled water was used to prepare the aqueous solutions.

2.2 Preparation of $Pd_1Ni_yAl_{0.5}$/MWCNTs nanoparticles

Firstly, 5.9 mg PdO and proper amounts of $NiCl_2{\cdot}4H_2O$ and Al_2O_3 were mixed with 20 mg MWCNTs in an agate mortar for 10 min, and then the mixture was ground for 15 min. And after that, 10 mL distilled water was added and sonicated for 40 min to generate a suspension solution. And then the well treated suspension solution was transferred into a home-made autoclave, and then the well-sealed autoclave was placed in a muffle furnace. The temperature of the muffle furnace was kept at 120 ºC for 3 h to finish the hydrothermal process, which was conducted in an SRJX-8-13 muffle furnace equipped with a KSY 12-16 furnace temperature controller. After cooling down to the room temperature naturally, the samples were filtered by distilled water and dried in ambient condition, leading to the formation of $Pd_1Ni_yAl_{0.5}$/MWCNTs catalysts. It should be mentioned that the amounts of $NiCl_2{\cdot}4H_2O$ and Al_2O_3 were weighed according to the atomic ratio of Pd:Ni:Al. The samples with the atomic ratios of Pd:Ni:Al amounting to 1:2:0.5,1:4:0.5 and 1:6:0.5, respectively, were denoted as sample **a**, **b** and **c**. The sample of Pd_1Ni_4/MWCNTs was also prepared using above process in the absence of Al_2O_3, being noted as sample **o**.

2.3 Preparation of $Pd_1Ni_yAl_{0.5}$/ MWCNTs modified GC electrode

Firstly, a glassy carbon (GC) electrode with a diameter of 3 mm was thoroughly polished using alumina nanopowder suspensions, and then the section of the well-polished GC electrode was

employed as a substrate. The working electrodes were prepared by dropping catalyst ink onto the sections of the well treated GC electrodes. The catalyst ink was fabricated by dispersing 1 mg catalyst into 1 mL Nafion ethanol solution (Nafion content was 0.1 wt.%). After 30 min ultrasonication, about 20 μL ink was dropped onto the surface of the sections of GC electrodes. Finally, the $Pd_1Ni_yAl_{0.5}$/MWCNTs-coated GC electrode was produced after drying in air conditions.

2.4 Characterizations

The morphologies of samples were examined by scanning electron microscopy (SEM, HITACHI, S-570) and transmission electron microscopy (TEM, HITACHI, H-7650). XRD analysis of the catalysts was carried out on a Bruker D8 ADVANCE X-ray diffractometer equipped with a Cu Kα source (λ= 0.154 nm) at 40 kV and 30 mA. The 2θ angular region between 10 and 90° was explored at a scan rate of 1°/step. Energy Dispersive X-Ray Spectroscopy (EDS) spectrum analysis was carried out on a X-ray energy instrument (EDAX, PV-9900, USA). Electrochemical measurements were carried out on a CHI 660B electrochemical working station (Shanghai Chenhua Apparatus, China) connected to a personal computer.

As prepared $Pd_1Ni_yAl_{0.5}$/MWCNTs modified GC electrode, a platinum wire and a saturated calomel electrode (SCE) were, respectively, utilized as the working electrode, counter electrode and reference electrode. All potentials in this work were reported with respect to the SCE electrode. A solution of 1 M KOH containing 1 M C_2H_5OH was used to study EOR activity. All the experiments were carried out at room temperature.

3. RESULTS AND DISCUSSION

3.1 XRD Analysis

The XRD patterns of the as-synthesized samples are illustrated in Fig. 1. For comparison, the XRD pattern for the pure MWCNTs was also displayed as shown by pattern **1**. Evidently, the diffraction peak appearing at around 26° can only be assigned to the (002) reflection of MWCNTs on the basis of our previous works concerning MWCNTs [15]. Additionally, for all other XRD patterns, except for the typical diffraction peaks of PdO, four characteristic reflection peaks, corresponding to the planes (111), (200), (220) and (311) of face centered cubic (fcc) crystalline Pd (JCPDS, Card No.01-089-4897), are vividly exhibited, being well consistent with the previous report [16]. This result strongly indicated that it was feasible to apply this simple method of hydrothermal process for synthesizing metallic Pd nanoparticles. After careful observation, the following conclusions could be obtained. First, although the diffraction peaks belonging to metallic Pd were observed in all the XRD patterns, the reflection peaks of PdO were still clearly displayed, which substantially demonstrated that the prepared samples were composites that contained PdO and metallic Pd. Second, the intensities of the diffraction peaks for the metallic Pd changed remarkably with the atomic ratios of Pd, Ni and Al in the starting materials. It indicated that the atomic ratio could affect the crystallinity of the prepared

metallic Pd. Third, no diffraction peaks of impurities such as nickel (or aluminum) oxide and nickel (or aluminum) hydroxide were presented, indicating the absence of those impurities.

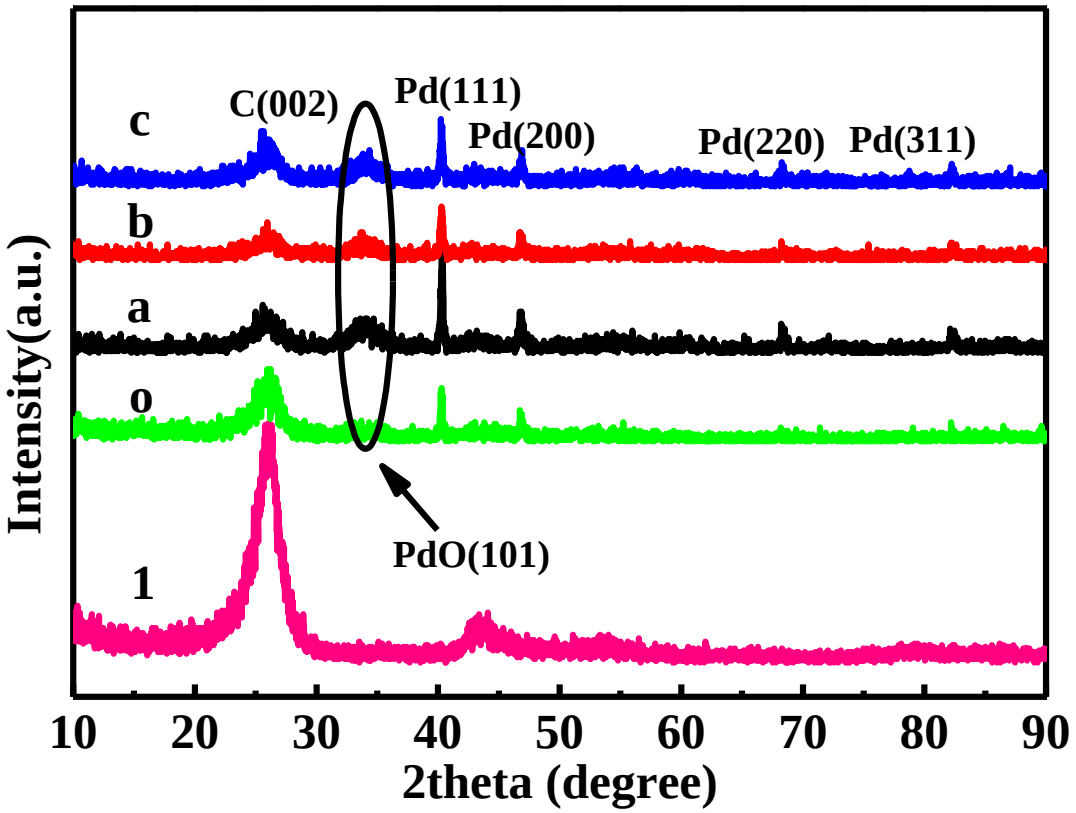

Figure 1. XRD patterns for the obtained samples of $Pd_1Ni_yAl_{0.5}$/MWCNTs. Pattern **a, b** and **c** correspond to $Pd_1Ni_2Al_{0.5}$, $Pd_1Ni_4Al_{0.5}$ and $Pd_1Ni_6Al_{0.5}$-coated MWCNTs. Pattern **1** and **o** correspond to the pure MWCNTs and Pd_1Ni_4-coated MWCNTs.

To further analyze the chemical composition of the as-prepared samples, EDS analysis was also performed. The typical EDS spectrum of the $Pd_1Ni_4Al_{0.5}$-coated MWCNTs was shown Fig. 2. Besides the peaks of carbon and oxygen, the peaks of metal elements Pd, Ni and Al are displayed clearly. Unfortunately, the atomic ratio of Pd:Ni: Al was 50.50: 1.14: 6.36, which did not accord with the atomic ratio in the precursors. Thus, the prepared samples should be the nominal particles of $Pd_1Ni_yAl_{0.5}$. Meanwhile, this result indicated that these three elements of Pd, Ni and Al all existed in the produced samples.

How did one comprehend the formation process of $Pd_1Ni_yAl_{0.5}$ composite particles? According to the previous study, prior to the utilization of MWCNTs, some organic groups like -OH,-COOH have been formed on the surface of MWCNTs due to the self-oxidation of MWCNTs [17].

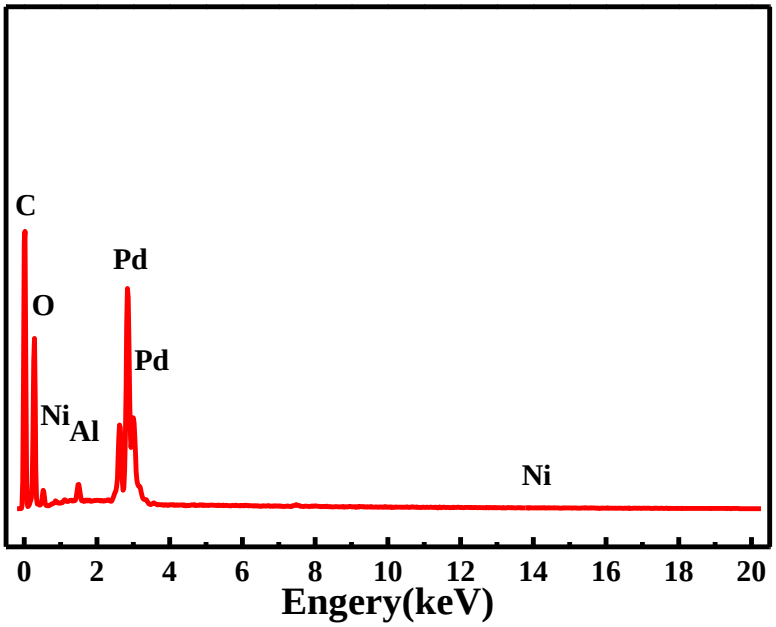

Figure 2. EDS spectrum for the typical catalyst of $Pd_1Ni_4Al_{0.5}$-coated MWCNTs.

These formed organic groups could react with the metal precursors in above hydrothermal process, leading to the generation of composite particles on the surface of MWCNTs. Meanwhile, in such a reacting system, MWCNTs may react with distilled water to produce some reductive gases like H_2 and CO, for instance, C +H_2O= H_2 +CO, according to the previous works concerning carbon [18]. That is to say, a reductive environment was produced in the preparing process due to the presence of MWCNTs. Furthermore, the standard electrode potentials of the starting metal precursors were different from each other. For example, the standard electrode potential of PdO ($E^{\theta}_{Pd^{2+}/Pd}$=0.915V vs. NHE) is much higher than that of $NiCl_2$ ($E^{\theta}_{Ni^{2+}/Ni}$= -0.257V vs. NHE) and Al_2O_3 ($E^{\theta}_{Al^{3+}/Al}$=-1.66V vs. NHE) [19], therefore, the reaction velocity of PdO should be much faster than $NiCl_2$ and Al_2O_3 when they reacted with the same reductant. As a result, more metallic Pd particles were formed first in above preparation process, and simultaneously, some metallic Ni and Al particles or their oxides were produced on the surface or internal part of Pd particles, leading to the formation of nominal trimetallic particles of $Pd_1Ni_yAl_{0.5}$.

3.2 Morphology characterization

The morphologies of the four prepared catalysts are displayed in Fig. 3. Obviously, for sample **b** and **c**, several huge irregular particles were anchored on the MWCNTs after the hydrothermal process. Furthermore, it seemed that some very small particles were immobilized on the surface of carbon nanotubes, which led to grey and black surface. This result implied that some substances were really prepared onto the surface of MWCNTs though some aggregates of particles were found in the prepared samples. Above observations effectively verified that the atomic ratio in the metal precursors was an important factor that could notably influence the morphologies of the resultant samples. To the

best of our knowledge, this is the first time to prepare the trimetallic particles of $Pd_1Ni_yAl_{0.5}$ and to present their SEM images.

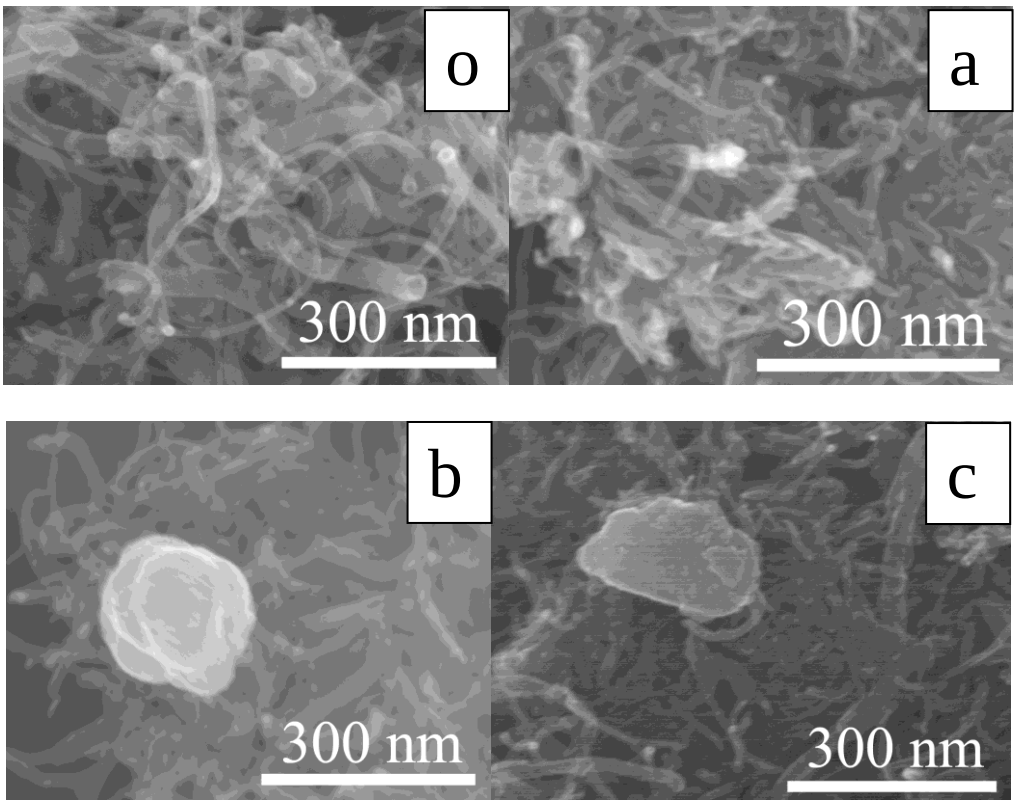

Figure 3. SEM images for the obtained samples of $Pd_1Ni_yAl_{0.5}$/MWCNTs. Image **o, a, b** and **c** correspond to Pd_1Ni_4/MWCNTs, $Pd_1Ni_2Al_{0.5}$/MWCNTs, $Pd_1Ni_4Al_{0.5}$/MWCNTs and $Pd_1Ni_6Al_{0.5}$/MWCNTs.

The TEM microstructures for these four samples are displayed in Fig. 4. Although several huge particles were seen on the surface of MWCNTs, the surface of MWCNTs were mainly coated by numerous small particles. Close observation revealed that the sizes of most small particles were less than 10 nm. And the particle sizes of the sample **o**, **a**, **b** and **c** were evaluated to be 7.42, 7.23, 5.78 and 7.56 nm, respectively, based on the TEM images. Evidently, the particle sizes observed in the SEM images were extremely larger than those displayed in the TEM images, which strongly indicated that those large particles appearing in Fig. 3 were constructed by many smaller particles. That is to say, aggregation occurred in the preparation process. Generally, smaller particle size was favorable for promoting the electrocatalytic activity of a catalyst especially when the loadings of catalysts were identical. Also, this is the first time to report the SEM and TEM images of trimetallic $Pd_1Ni_yAl_{0.5}$ composite nanoparticles, to our knowledge.

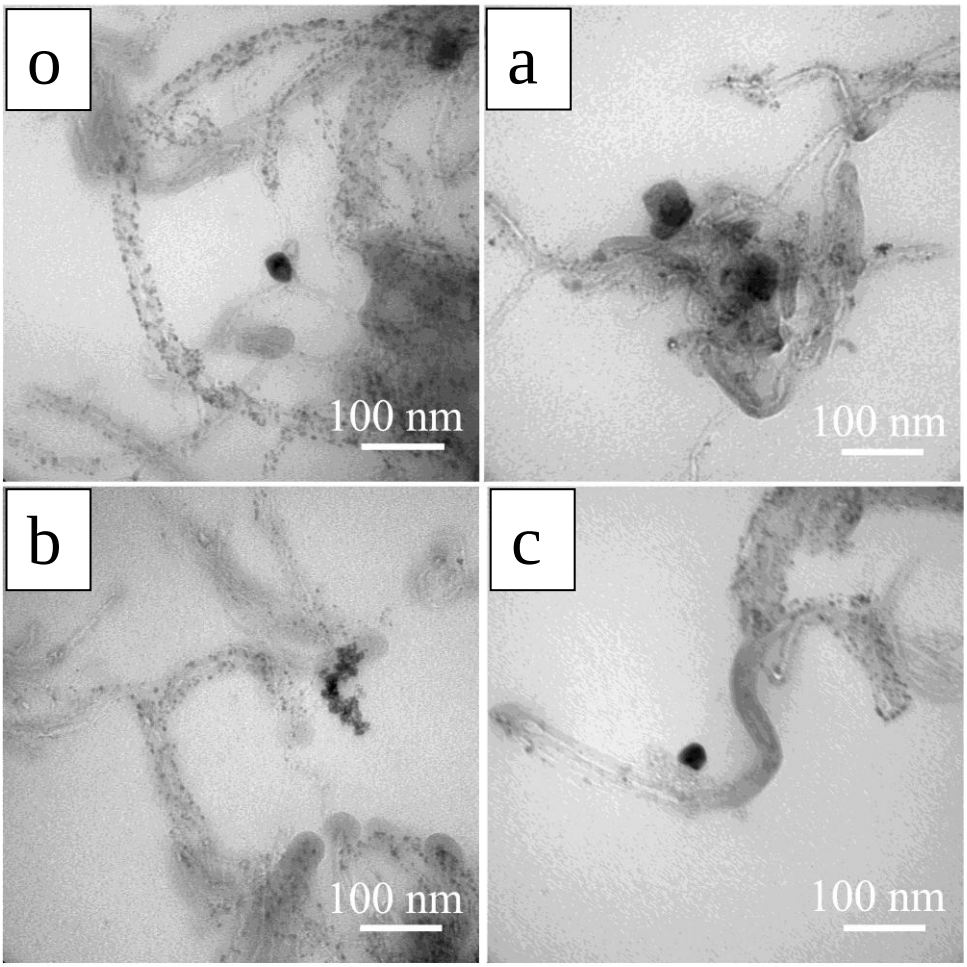

Figure 4. TEM images for the obtained samples of $Pd_1Ni_yAl_{0.5}$/MWCNTs. Image **o**, **a, b** and **c** correspond to Pd_1Ni_4, $Pd_1Ni_2Al_{0.5}$, $Pd_1Ni_4Al_{0.5}$ and $Pd_1Ni_6Al_{0.5}$-coated MWCNTs.

3.3. Electrochemical characterization

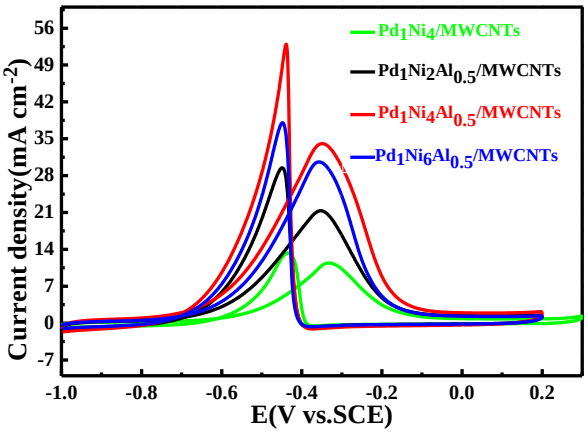

Figure 5. Cyclic voltammograms (CVs) obtained on the $Pd_1Ni_yAl_{0.5}$/MWCNTs-coated GC electrodes in 1M KOH having 1M C_2H_5OH solution at the scan rate of 50 mV s^{-1}. The green, black, red and blue curves were measured on the Pd_1Ni_4, $Pd_1Ni_2Al_{0.5}$, $Pd_1Ni_4Al_{0.5}$ and $Pd_1Ni_6Al_{0.5}$-coated MWCNTs catalysts.

The cyclic voltammograms (CVs) of the $Pd_1Ni_yAl_{0.5}$/MWCNTs catalysts in a solution of 1 M KOH containing 1M C_2H_5OH were recorded at the scan rate of 50 mV s^{-1} and presented in Fig. 5. For all the catalysts, one oxidation peak positioned at ~-0.35 V in the anodic sweep curve and one centered at ~-0.45 V in the cathodic sweep were exhibited clearly. The shapes of these CV cyrves were very similar to those measured on the Pd-coated GC electrode [20]. CV curves in Fig. 5 substantially indicated that all the prepared catalysts could be used as electrocatalysts for EOR in alkaline media. As shown by the red line, the highest peak current density of EOR was found on the catalyst of $Pd_1Ni_4Al_{0.5}$/MWCNTs, which verified that $Pd_1Ni_4Al_{0.5}$/MWCNTs possessed the best electrocatalytic activity for EOR when compared to other catalysts. Moreover, this result demonstrated that the atomic ratio of Pd, Ni and Al in the resultant samples played an important role in deciding the final electrocatalytic activity of the resultant trimetallic nanoparticle catalysts. As shown in Fig.4, probably, the smaller particle size of $Pd_1Ni_4Al_{0.5}$ may account for its excellent electrocatalytic activity, since the contacting area between the electroactive materials (ethanol) and electrode would be significantly augmented when the particle size of catalysts were reduced.

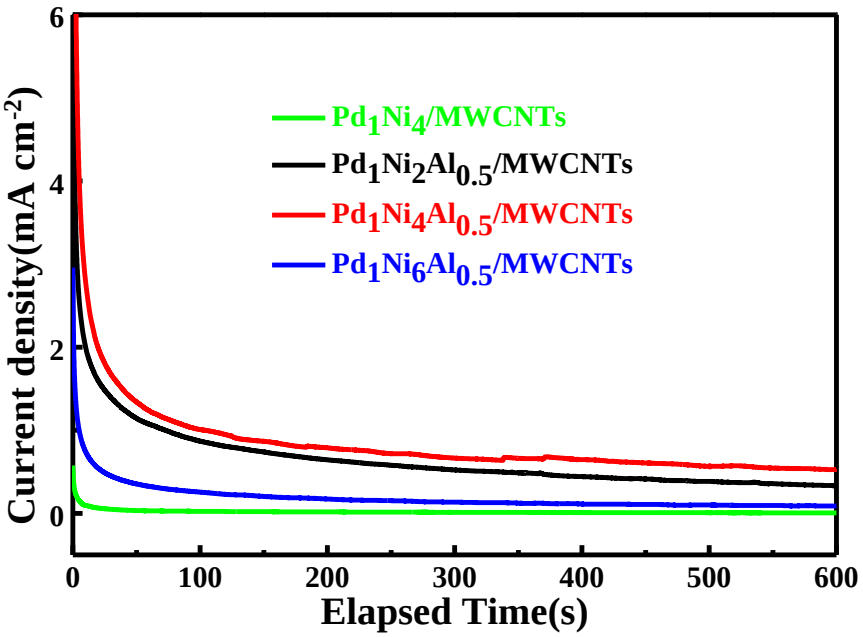

Figure 6. Chronoamperometry curves of the as-prepared electrodes recorded in 1M KOH +1M C_2H_5OH at -0.24 V. The green, black, red and blue curves were measured on the Pd_1Ni_4, $Pd_1Ni_2Al_{0.5}$, $Pd_1Ni_4Al_{0.5}$ and $Pd_1Ni_6Al_{0.5}$-coated MWCNTs catalysts.

To further examine the electrochemical stability of all the prepared catalysts towards EOR, chronoamperometric (CA) curves of the $Pd_1Ni_yAl_{0.5}$/MWCNTs-modified GC electrodes at -0.24 V in 1 M KOH + 1M C_2H_5OH were measured as shown in Fig. 6 [20]. All the curves displayed a sharp decrease of the current density in the initial stage and a relatively stable current density in the left testing period. Commonly, the sharply decreased current was related to the electric double layer of an electrode, and the relatively stable current was attributed to the polarized current (Faradaic current). Or in other words, the stable current was mainly from the electro-oxidation of ethanol and its oxidation

intermediates. Apparently, the catalyst of $Pd_1Ni_4Al_{0.5}$ delivered the largest current density in the testing period. For example, the current densities at the catalysts of $Pd_1Ni_2Al_{0.5}$, $Pd_1Ni_4Al_{0.5}$ and $Pd_1Ni_6Al_{0.5}$ were about 0.34, 0.51 and 0.08 mA cm^{-2} at 600 s, respectively. While for the Pd_1Ni_4 catalyst, the polarized current was close to zero at the testing time of 600 s. This result attested that the catalyst of $Pd_1Ni_4Al_{0.5}$/MWCNTs exhibited not only the highest polarized current density but also the best stability and durability among all the synthesized catalysts when employed as a catalyst towards EOR. Also, this result indicated that doping a proper amount of Al into the Pd-Ni bimetallic catalyst was helpful to improve the electrocatalytic activity of Pd-Ni catalysts.

3.4. Electrocatalytic mechanism analysis

Why did the trimetallic $Pd_1Ni_yAl_{0.5}$ nanoparticle catalysts with different metal molar ratios show such different electrocatalytic activity for EOR? To uncover the possible reasons, the curves of open circuit potentials against time for the three typical electrodes in 1 M KOH were illustrated in Fig. 7.

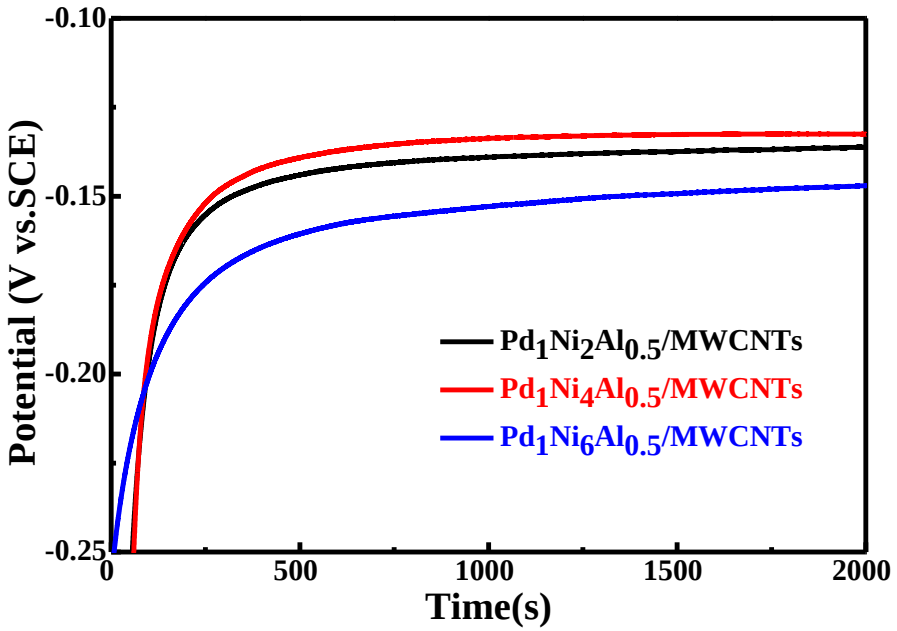

Figure 7. The curves of open circuit potentials against time for three typical electrodes which were recorded in 1M KOH solution. The black, red and blue curves corresponded to the $Pd_1Ni_2Al_{0.5}$, $Pd_1Ni_4Al_{0.5}$ and $Pd_1Ni_6Al_{0.5}$-coated MWCNTs modified GC electrodes.

Fig. 7 shows the relationship of open circuit potential (OCP) between the testing time. A sharp increase of OCP value was observed for these three catalysts within the initial period time of around 360 s. And then, the values of OCP for all the three electrodes reached a stable status after a certain period. According to the theory of Nernst equation [21], the OCP value of an electrode was mainly determined by its nature, though the concentration of ions and the surface structure could also

influence the value of OCP. Evidently, the stable values of OCP for these three electrodes were different, that is to say, the contents of Pd, Ni and Al in the prepared catalysts had greatly influenced the OCP value. For example, at the duration time of 2000 s, the values of COP for the catalysts **a**, **b** and **c** were about -0.136, -0.132 and -0.147V, respectively. That is to say, the highest value of OCP was presented by the catalyst of $Pd_1Ni_4Al_{0.5}$. This result suggested that the electro-oxidation ability of $Pd_1Ni_4Al_{0.5}$ was superior to other catalysts based on the Nernst Equation [21], thus, probably ethanol molecules and the intermediates formed in the electrooxidation of ethanol process were easier to be electro-oxidized on the catalyst of $Pd_1Ni_4Al_{0.5}$ when compared to other catalysts.

To further study the electrocatalytic mechanism of the as-prepared catalysts for the EOR in alkaline media, chronopotentiometry (CP) tests [22] were carried out and the results are given in Fig. 8. In the CP tests, a constant current density of 0.14 mA cm^{-2} was applied on the electrodes for 12000 s. According to the electrochemical theory, the electrode potential would increase when being applied with a positive current. For all the electrodes, the polarized electrode potentials were increased sharply in the initial stage and then relatively stable values were attained. Although all CP curves showed similar shapes, the stable values of electrode potential for these three catalysts were varied from each other. At the end of testing period of 12000 s, the values of electrode potentials for the catalysts **a**, **b** and **c** were about 0.30, 0.35 and 0.28V, respectively. Thus, the highest value of electrode potential was still displayed by the catalyst of $Pd_1Ni_4Al_{0.5}$, indicating that electro-oxidation ability of $Pd_1Ni_4Al_{0.5}$ was much higher than other catalysts. Meanwhile, the fact, that the polarized electrode potentials were rather different from each other, also indicated that the composition of these three catalysts were different, which was consistent with the results obtained from XRD and EDS measurements.

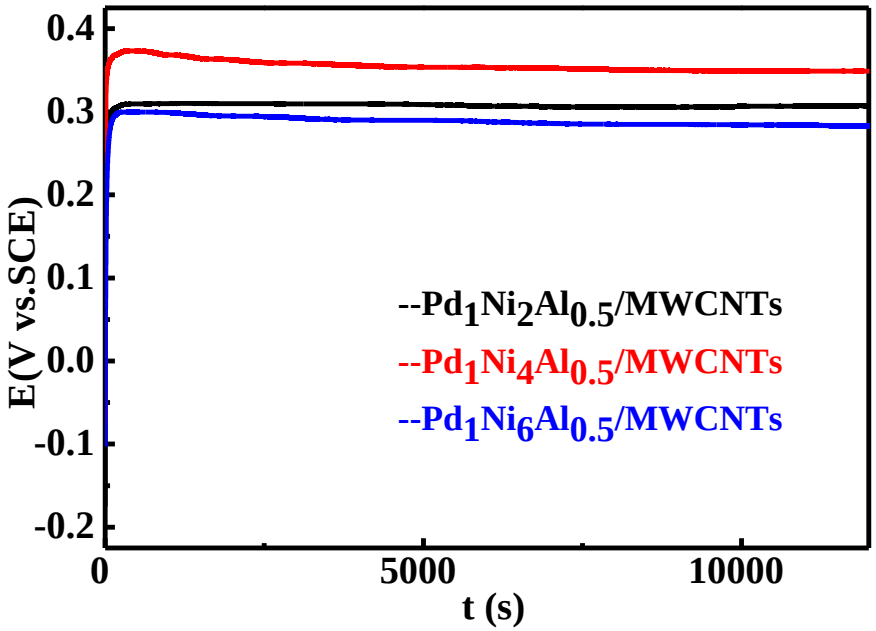

Figure 8. Chronopotentiometric curves of $Pd_1Ni_yAl_{0.5}$/MWCNTs coated GC electrode in 1 M KOH+1 M C_2H_5OH solution with the applied current density of 0.14 mA cm^{-2}. The black, red and blue curves corresponded to the $Pd_1Ni_2Al_{0.5}$, $Pd_1Ni_4Al_{0.5}$ and $Pd_1Ni_6Al_{0.5}$-coated MWCNTs electrodes.

As one typical curve of electrochemical impedance spectroscopy (EIS), Bode plot has been widely used to acquire more information on the electrical properties of a catalyst [23]. Bode plots for the three catalysts are illustrated in Fig. 9. It can be seen clearly that all the three catalysts coated GC electrodes showed a symmetric peak in the whole frequency region, which was originated from the relaxation process of the electrode|solution interface [24]. The phase angles at 0.02Hz for the **a**, **b** and **c** electrodes were approximately -77º, -78º and -82º, respectively. Generally, an ideal capacitive system usually gives a phase angle of *ca.* −90º [24] in the Bode plot at the lowest frequency value, thus, all these three catalysts modified electrodes could be regarded as quasi-capacitors. Careful observation revealed that there were two arcs for the $Pd_1Ni_4Al_{0.5}$/MWCNTs-coated GC electrode in the frequency region from 0.1 to 500 Hz. This result indicted that there were two kinds of interfaces of electrode|solution in the case of $Pd_1Ni_4Al_{0.5}$/MWCNTs-coated GC electrode. Although the exact structures of these three electrodes cannot be revealed by using the Bode plot simply, it can be confirmed that the surface structure of the $Pd_1Ni_4Al_{0.5}$/MWCNTs-coated GC electrode was rather different from the other two electrodes.

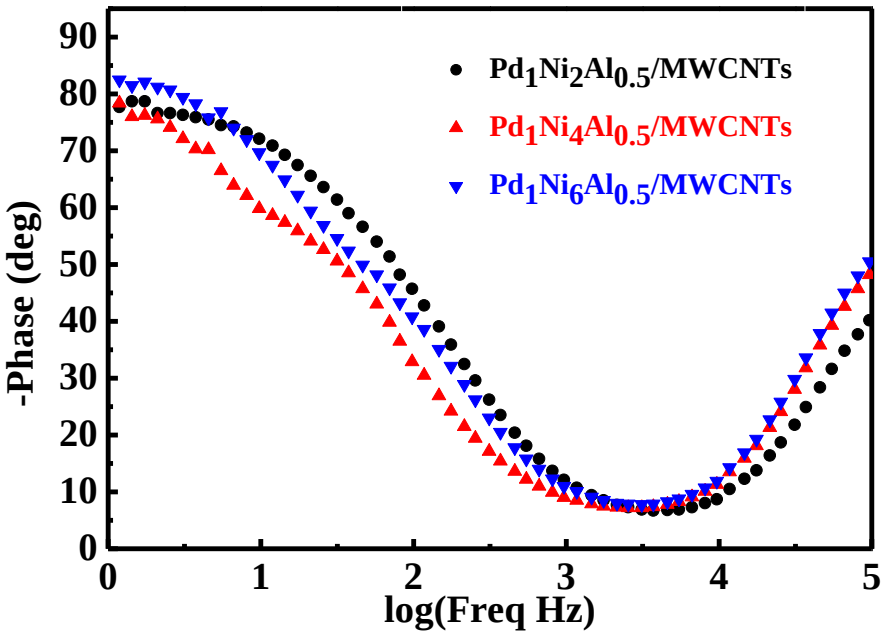

Figure 9. Bode plots obtained at open circuit potentials for the catalysts coated GC electrodes in 1 M KOH+1 M C_2H_5OH aqueous solution.

4. CONCLUSION

For the first time, trimetallic $Pd_1Ni_yAl_{0.5}$ nanoparticle catalysts with various atomic ratios were prepared by a hydrothermal process in the presence of metal precursors, distilled water and MWCNTs. The results obtained from XRD characterization demonstrated that the main components of the resulting samples were PdO and metallic Pd, though nickel and aluminum salts were contained in the starting materials. Results from SEM and TEM observation indicated that the atomic ratio of metals in the precursors played a key role in affecting the morphologies of resultant samples and determining the particle sizes of resulting catalysts. It was thought that the relatively higher value of OCP, the higher

polarized electrode potential and the particular surface structure should be responsible for the excellent electrocatalytic performance of $Pd_1Ni_4Al_{0.5}$/MWCNTs towards EOR when compared to other catalysts synthesized in this work. Presenting a novel electrocatalyst of trimetallic $Pd_1Ni_yAl_{0.5}$ nanopaticle for EOR as well as showing the preparation method of hydrothermal process is the main contribution of this preliminary work, which will be beneficial to the development of electrocatalysts for EOR.

ACKNOWLEDGEMENTS
This work was financially supported by the National Natural Science Foundation of China (No. 21173066), Natural Science Foundation of Hebei Province of China (No.B2015205150; No.B2011205014).

References

1. T. Hua, R. Ahluwalia, L. Eudy, G. Singer, B. Jermer, N. Asselin-Miller, S. Wessel, T. Patterson and J. Marcinkoski, *J. Power Sources*, 269 (2014) 975.
2. W. Du, G. Yang, E. Wong, N. Aaron Deskins, A. I. Frenkel, D. Su and X. Teng, *J. Am. Chem. Soc.*, 136 (2014) 10862.
3. H. Y. Na, L. Zhang, H. Qiu, T. Wu, M. Chen, N. Yang, L. Li, F. Xing and J. Gao, *J. Power Sources*, 288 (2015) 160.
4. N. Tian, Z. Y. Zhou, S. G. Sun, Y. Ding and Z. L. Wang, *Science*, 316 (2007) 732.
5. Ali A. Ensafi, M. Jafari-Asl, B. Rezaei, M. Mokhtari Abarghoui and H. Farrokhpour, *J. Power Sources*, 282(2015) 452.
6. C. V. Rao and B. Viswanathan, *Electrochim. Acta*, 55 (2010) 3002.
7. H. An, H. Cui, D. Zhou, D. Tao, B. Li, J. Zhai and Q. Li, *Electrochim. Acta*, 92 (2013) 176.
8. M. Soszko, M. Łukaszewski, Z. Mianowska and A. Czerwiński, *J. Power Sources*, 196 (2011) 3513.
9. X. Lu, F. Luo, H. Song, S. Liao and H. Li, *J. Power Sources*, 246 (2014) 659.
10. 10. T.S. Almeida, A.R. Van Wassen, R.B. VanDover , A.R. de Andrade and H.D. Abruňa, *J. Power Sources*, 284 (2015) 623.
11. H. Yin, P. Chen, C. Xu, X. Gao, Q. Zhou, Y. Zhao and L. Qu, *Carbon*, 94 (2015) 928.
12. A. Simon, M. Seyring, S. Kämnitz, H. Richter, I. Voigt, M. Rettenmayr and U. Ritter, *Carbon*, 90 (2015) 25.
13. Y. Zhao, L. Fan, Y. Zhang, Q. Que and B. Hong, *J.Power Sources*, 296 (2015)30.
14. K. Ding, Y. Zhao, L. Liu, Y. Cao, Q. Wang, H. Gu, X. Yan and Z. Guo, *Int. J. Hydrogen Energ.*, 39 (2014) 17622.
15. K. Ding and M. Cao, *Russ. J. Electrochem.*, 44 (2008) 977.
16. K. Ding, L. Liu, Y. Cao, X. Yan, H. Wei and Z. Guo. *Int. J. Hydrogen Energ.*, 39 (2014) 7326.
17. H.P. Boehm, Chemical identification of surface groups. In: Advances in catalysis, 16. New York: Academic Press; 1966. p. 179.
18. Z. Zhu, G.Q. Lu, J. Finnerty and R.T. Yang. *Carbon* 41 (2003) 635.
19. A. J. Bard and L.R. Faulkner, *Electrochemical methods fundamentals and applications*, 2nd Edition. Published By John Wiley& Sons, Inc. 2001
20. K. Ding, Y. Li, Y. Zhao, L. Liu, H. Gu, L. Liu, S. Qiu, C. He , J. Liu, Q. Wang and Z. Guo, *Electrochim. Acta*, 149 (2014) 186.
21. P. Ju, Y. Zuo, Y. Tang and X. Zhao. *Corros. Sci.*, 66 (2013) 330.
22. T. H. T. Vu, T. T. T. Tran, H. N. T. Le, L. T. Tran, P. H. T. Nguyen and N. Essayem *J. Power Sources*, 276 (2015) 340.

23. L. Liu, J. Wang, H. Wei, Z. Guo and K. Ding, *Int. J. Electrochem. Sci.,* 9 (2014) 2221.
24. C. Hu, S. Yuan and S. Hu, *Electrochim. Acta,* 51(2006) 3013.